

# Blue Stragglers as Stellar Collision Products: the Angular Momentum Question

Alison Sills<sup>1</sup>, Tim Adams<sup>2</sup> and Melvyn B. Davies<sup>3,2</sup>

<sup>1</sup>*Department of Physics and Astronomy, McMaster University, Hamilton, Ontario, Canada L8S 4M1*

<sup>2</sup>*Department of Physics and Astronomy, University of Leicester, Leicester, LE1 7RH*

<sup>3</sup>*Lund Observatory, Box 43, SE-221 00, Lund, Sweden*

Received \*\* \*\*\* 2004; in original form 2004 \*\*\* \*\*

## ABSTRACT

We investigate the structure and evolution of blue stragglers stars which were formed from direct stellar collisions between main sequence stars in globular clusters. In particular, we look at the rotational evolution of the products of off-axis collisions. As found in previous work, such blue stragglers initially have too high an angular momentum to contract down to the main-sequence. We consider angular momentum loss through either disc locking or locking to an outflowing wind and show that both methods allow the merged object to shed sufficient angular momentum to contract down to the main-sequence.

**Key words:** convection – hydrodynamics – blue stragglers – stars: rotation

## 1 INTRODUCTION AND MOTIVATION

Blue stragglers are those main sequence stars which are bluer and brighter than the main sequence turnoff in clusters, and must therefore be younger than the bulk of the cluster population. In globular clusters especially, which are devoid of an interstellar medium from which to form young stars, two viable mechanisms for blue straggler formation exist.

First, blue stragglers could be a result of a collision between two main sequence stars. Globular clusters are crowded places, with densities in post-core-collapse clusters in excess of  $10^5$  stars/pc<sup>3</sup>. Within such a crowded environment it is inevitable that collisions will occur between stars. Indeed collisions have been invoked as a possible mechanism for explaining the apparent paucity of red giants in the cores of globular clusters (Adams, Davies, & Sills 2004). It seems reasonable that collisions could play a role in the creation of blue stragglers.

In Fig. 1 We plot the normalised collision probability for the  $0.4 M_{\odot}$  model used throughout this work (Bailey & Davies 1999). The other stellar models follow a similar path. As can be seen in this figure, the vast majority of collisions are likely to occur for a star whilst it is on the main-sequence. This is simply because the main-sequence lifetimes of these low mass stars is very long.

Alternatively, blue stragglers may be formed within primordial binaries. Preston & Sneden (2000) describe observations of blue stragglers observed in the field. They conclude that they must be produced by a period of mass transfer within a binary system. Mass from the more evolved star can pass to the less evolved companion as it expands and

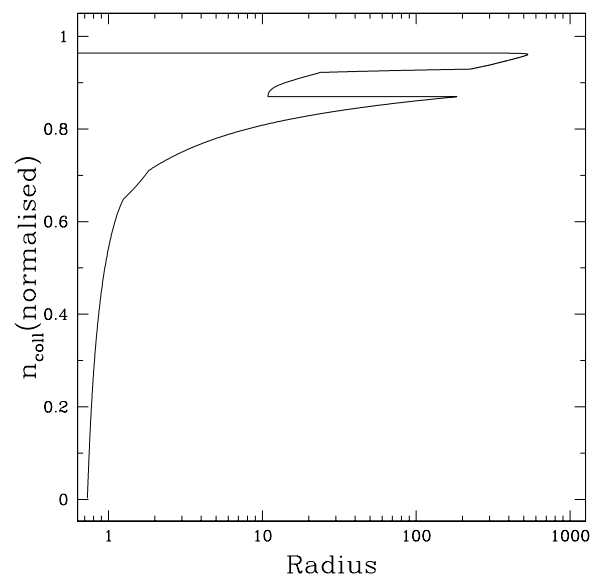


**Figure 1.** The normalised collision probability for the  $0.4 M_{\odot}$  model used in this investigation as a function of its radius (which is a tracer of its age). As can be seen the star is most likely to undergo a collision while it is on the main-sequence. The paths for the  $0.6$  and  $0.8 M_{\odot}$  models are very similar to this.

fills its Roche lobe. The impact of such primordial systems on the entire blue straggler population within a globular cluster is discussed in Davies *et al.* (2004).

We currently do not have good diagnostics to discriminate between collisional blue stragglers and binary mergers observationally. A number of groups have modelled direct physical collisions between main sequence stars (Benz & Hills 1987; Lombardi *et al.* 1996; Sandquist *et al.* 1997; Sills *et al.* 2001) and the subsequent evolution of the collision products (Sills *et al.* 1997, 2001) to investigate positions in the colour-magnitude diagram, rotation rates and surface abundances. The equivalent work has not yet been done for binary mergers. This is mostly because of the difficulty is following the evolution of a hydrodynamic system (the mass transfer between binary components) for the length of time required for the system to merge. This timescale is unknown but certainly large, on the order of half a billion years (e.g. Rahunen 1981).

The details of the evolution of blue stragglers from either formation mechanism is both interesting in its own right, and necessary for detailed studies of the dynamics of globular clusters. Over the last decade, it has become more obvious that dynamical models of globular clusters needed to incorporate more realistic stellar effects. Rather than treating the cluster as a self-gravitating system of equal-mass point masses, the stars in the cluster were allowed to have a spectrum of masses. This required some discussion of stellar evolution, so that high mass stars were not still influencing the dynamics of the cluster well after they had evolved off the main sequence. Binary stars, particularly primordial binaries, became critically important for halting core collapse in clusters, necessitating some form of binary evolution in the dynamics codes. Stars were also given finite radii, which allowed the study of stellar collisions. All these new levels of complexity point in one direction – understanding the interplay between stellar dynamics and stellar evolution is an essential component in understanding globular clusters and their populations.

Stellar collisions are one component of this problem, and fortunately, the products of some stellar collisions are readily observed in the colour-magnitude diagram as blue stragglers. Therefore, by understanding the current population of blue stragglers in clusters, we can begin to probe the past dynamical history of the cluster. This is particularly true if we limit ourselves to regions of the cluster where collisions are likely to dominate (i.e. the centres of dense clusters), which has been possible since the advent of the Hubble Space Telescope. We have made some comparisons between HST observations and theoretical predictions in a number of clusters (Sills & Bailyn 1999; Sills *et al.* 2001; Ferraro *et al.* 2003). In order to make these comparisons, we need to understand the evolution of blue stragglers in the colour magnitude diagram over their entire lifetimes.

In previous work, we used the results of smoothed particle hydrodynamics (SPH) simulations of stellar collisions as starting models of stellar evolution calculations, and we produced detailed evolutionary models for a variety of collision products relevant to globular clusters. For head-on collisions at both medium and high SPH resolution (Sills *et al.* 1997; Sills, Adams, Davies, & Bate 2002), these models were very successful, and we understand the evolution of these collision products quite well. However, the limiting case of exactly head-on collisions is unrealistic. Most collisions will have some non-zero impact parameter. These off-axis collision products have substantial angular momentum from their

initial configuration (even assuming initially non-rotating stars). Even a collision with a very small, but non-zero impact parameter can result in a collision product with substantial angular momentum. This poses a problem for the subsequent evolution of the blue straggler.

It has been known for some time that immediately after the collision, the stars are rotating quite rapidly (Lombardi *et al.* 1996). They have total angular momenta up to 10 times larger than low-mass pre-main sequence stars ( $\sim 10^{51}$  g cm<sup>2</sup> s<sup>-1</sup> for the collision products), and, like pre-main sequence stars, have very large radii. Therefore, they are rotating rapidly, but not unduly so. Like pre-main sequence stars, the collision products evolve by contracting towards the main sequence. Unlike pre-main sequence stars, however, collision products do not have surface convection zones, and therefore cannot lose angular momentum via a magnetic wind (Chaboyer, Demarque, & Pinsonneault 1995). The contraction of a pre-main sequence star combined with this wind loss results in a normal main sequence star with approximately 1% of its initial angular momentum. The contraction of a collision product without this wind loss results in a star which is rotating at greater than its break-up velocity long before it reaches the main sequence. The conclusion of Sills *et al.* (2001) was that either blue stragglers cannot be created by stellar collisions because they tear themselves apart through rapid rotation, or that some other mechanism for removing angular momentum must occur.

Very little observational data exists for rotation rates of blue stragglers. The only blue stragglers in a globular cluster to have its rotation rate measured are BSS 19 in 47 Tucanae (Shara *et al.* 1997), which has  $v \sin i = 155 \pm 55$  km s<sup>-1</sup>; and M3-17 (De Marco *et al.* 2004) with  $v \sin i = 200 \pm 50$  km s<sup>-1</sup>. There is also an upper limit of  $v \sin i = 50$  km s<sup>-1</sup> on NGC6752-11 (De Marco *et al.* 2004). The other blue stragglers with measured rotation rates are found in the old open cluster M67 (Peterson *et al.* 1984). These stars have  $v \sin i$  between 10 and 120 km s<sup>-1</sup>, which is somewhat lower than most stars of the same temperature in younger clusters. Most of the blue stragglers in M67 are found in binary systems, which may indicate that their formation mechanism is different from those in globular clusters. The lack of observation of rotation velocities for globular cluster blue stragglers means that we cannot directly compare our predictions of rotation rates with data. Instead, we are restricted to looking at the effect of rotation on the position of stars in the colour-magnitude diagram, and making inferences about what is plausible.

Very recently, some interesting observational results have been published which may shed new light on this problem. De Marco *et al.* (2004) have discovered very sparse circumstellar discs around six blue stragglers in globular clusters, out of the 55 or so for which they have HST/STIS spectra. Since magnetic locking of the star to a disc is the leading mechanisms for angular momentum loss in these systems, this result is encouraging. Four of the six blue stragglers have no measure rotation rates. In this small sample, there is not enough information to place strong constraints on models yet.

In this paper, we revisit the question of structure and evolution of collision products. In particular we restrict ourselves to off-axis collisions between main sequence stars relevant to globular clusters. We concentrate on investigating a

plausible mechanism for removing angular momentum from the collision products early in their post-collision evolution. Section 2 describes the simulations of the collisions themselves, while section 3 outlines our approach to the evolution of the collision products and how the angular momentum evolution is treated. Section 4 draws conclusions based on these calculations and discusses how these results may impact our understanding of blue straggler populations in globular clusters.

## 2 SMOOTHED PARTICLE HYDRODYNAMICS SIMULATIONS

### 2.1 Method

The simulations of stellar collisions discussed in this paper are very similar to those presented in Sills, Adams, Davies, & Bate (2002). We used the smoothed particle hydrodynamics technique (Benz 1990; Monaghan 1992). Our three-dimensional code uses a tree to solve for the gravitational forces and to find the nearest neighbours (Benz 1990). We use the standard form of artificial viscosity with  $\alpha = 1$  and  $\beta = 2.5$  (Monaghan 1992), and an adiabatic equation of state. The thermodynamic quantities are evolved by following the change in internal energy. Both the smoothing length and the numbers of neighbours can change in time and space. The smoothing length is varied to keep the number of neighbours approximately constant ( $\sim 50$ ). The code is the parallel version of the code described in Bate, Bonnell & Price (1995) It was parallelized using OpenMP, and was run on the SGI Origin 3800 operated by the UK Astrophysical Fluids Facility (UKAFF) based at the University of Leicester, and on the SHARCNet facilities at McMaster University.

We modelled collisions between main sequence stars of masses 0.4, 0.6 and 0.8  $M_{\odot}$  with impact parameters between 0.25 and 1 in units of the sum of the parent star radii, as outlined in Table 1. The initial stellar models were calculated using the Yale stellar evolution code (YREC, (Guenther *et al.* 1992)) and had a metallicity of  $Z=0.001$  and an age of 13.5 Gyr. This age was chosen so that the 0.8  $M_{\odot}$  star was just at the turnoff. The particles were initially distributed on an equally spaced grid, and their masses were varied until the density profile matched that of the stellar model. The outermost SPH particles were set so that they were within one smoothing length of the outer radius of the star as calculated by YREC. This positioning of the particles and the variable particle masses were chosen in order to resolve the majority of the star, including particularly the outer layers. The stars were given a relative velocity at infinity of  $v_{\infty}=10 \text{ km s}^{-1}$ , which is a reasonable value for globular cluster stars. They were set up on almost parabolic orbits with a pericentre separation as shown in Table 1. The stars are initially non-rotating and separated by 5  $R_{\odot}$ . The centre of mass of the system is set to be at the origin.

### 2.2 Results

The global properties of our collision products agree with those presented in Sills *et al.* (2001) for those simulations

**Table 1.** Description of SPH simulations performed

Run name	m1 $M_{\odot}$	m2 $M_{\odot}$	rp r1+r2	Npart	r1 $R_{\odot}$	r2 $R_{\odot}$
M44Q	0.4	0.4	0.25	69 464	0.40	0.40
M44H	0.4	0.4	0.5	86 784	0.40	0.40
M44F	0.4	0.4	1.0	100 994	0.40	0.40
M46Q	0.4	0.6	0.25	44 702	0.40	0.61
M46H	0.4	0.6	0.5	36 750	0.40	0.61
M48Q	0.4	0.8	0.25	100 514	0.40	1.15
M66Q	0.6	0.6	0.25	100 034	0.61	0.61
M66H	0.6	0.6	0.5	100 034	0.61	0.61
M66F	0.6	0.6	1.0	100 034	0.61	0.61
M68Q	0.6	0.8	0.25	100 034	0.61	1.15
M88Q	0.8	0.8	0.25	100 034	1.15	1.15

with the same initial conditions. In Table 2 we give some information about the final state of each collision. In column 2 we give the total angular momentum of the collision product. In column 3 we give the ratio of the rotational energy about the z axis (T) to the potential energy (W) of the system. A rotating system is considered to be secularly unstable if  $T/|W| \geq 0.14$ , and dynamically unstable if  $T/|W| \geq 0.26$  (Tassoul 2000). All our collision products begin their lives considerably below these values. In column 4 we give the mass of the collision product immediately after the collision. For a given choice of parent masses, the mass loss due to the collision is larger for smaller impact parameters.

In Fig. 2 we show a time series plot from a collision between a 0.6 and a 0.4  $M_{\odot}$  star with a minimum distance of approach of  $0.25(R_1+R_2)$ . As was found in previous work, it is the material with the highest entropy (in most cases, this is the material from the most evolved star) which ends up at the centre of the blue straggler. However, there is some mixing of material and some of the material from the less evolved star does make it into the core of the collision product. A similar pattern is found in all of the collisions.

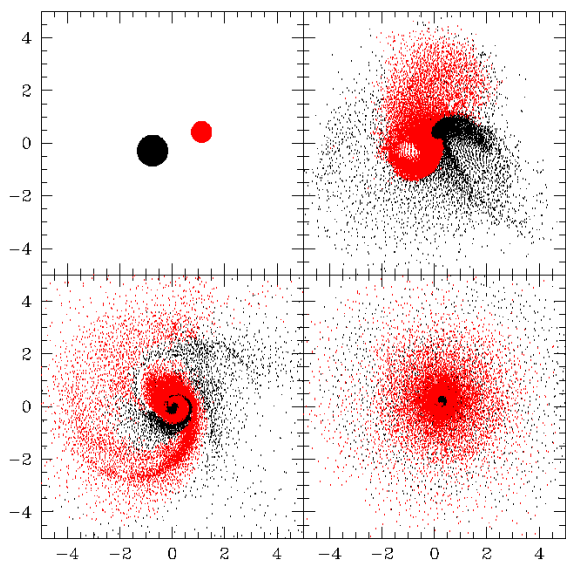
This is again present in Fig. 3. Here we have plotted a histogram similar to that shown in Benz & Hills (1987). The different levels of shading represent where material has come from within the star. All the stars are split into four bins based on radius from their centres. Where the material ends up in the bins of the blue straggler is then shown in the bottom histogram. The heaviest shading represents the material from the inner quartile of the parent stars, whilst the lightest shading represents the outermost quartile. Again we can clearly see that the inner regions of the blue straggler are made up the material from the innermost regions of the parent stars, and thus the blue straggler is not well mixed. This is most true of the head-on collision, but still quite apparent in the offaxis collision.

Figure 4 shows the structure of off-axis collision products between two 0.6  $M_{\odot}$  stars with a variety of impact parameters. The biggest difference between the three different collision products is their internal rotation rates. For the most part, their structural parameters are very similar.

Figure 5 gives the angular velocity of each SPH particle in the M44F collision as a function of mass fraction. There are two important things to be noticed in this figure. First, the SPH particles form a very tight sequence, indicating that when we transform from our inherently 3-D

**Table 2.** Results of SPH simulations.

Run name	J g cm <sup>2</sup> s <sup>-1</sup>	T/ W	M <sub>final</sub> M <sub>⊙</sub>
M44Q	6.96 × 10 <sup>50</sup>	0.038	0.748
M44H	9.85 × 10 <sup>50</sup>	0.067	0.772
M44F	9.89 × 10 <sup>50</sup>	0.069	0.796
M46Q	1.03 × 10 <sup>51</sup>	0.033	0.856
M46H	1.48 × 10 <sup>51</sup>	0.039	0.836
M48Q	1.58 × 10 <sup>51</sup>	0.001	1.06
M66Q	1.11 × 10 <sup>51</sup>	0.026	1.16
M66H	1.57 × 10 <sup>51</sup>	0.047	1.17
M66F	2.22 × 10 <sup>51</sup>	0.052	1.19
M68Q	2.32 × 10 <sup>51</sup>	0.038	1.37
M88Q	3.34 × 10 <sup>51</sup>	0.008	



**Figure 2.** A time series plot of those particles contained within  $2h$  of the  $z=0$  plane. This is a collision between a  $0.6$  (black particles) and a  $0.4$   $M_{\odot}$  (red particles) star, with a minimum distance of approach of  $0.255 R_{\odot}$  (i.e.  $0.25 R_1 + R_2$ ). As can be seen, it is the material from the heavier star which ends up at centre of the merged object. It is the composition of the core which will determine how long a particular blue straggler will spend on the main sequence compared to a star of the same mass produced through the collapse of the initial gas cloud.

SPH simulation to our inherently 1-D stellar evolution calculation, we have correctly identified the axis of rotation of the collision product, and that the collision product is rotating in a coherent manner. Secondly, the angular velocity of this collision product (and all the products produced in these simulations) is almost constant for a large fraction of the interior of the star. While similar simulations show a reasonably flat omega profile (Sills *et al.* 2001), the profiles derived from these simulations are even flatter. This is probably because of our use of the Monaghan artificial viscosity, which is known to introduce some shear viscosity that will artificially flatten rotation profiles.

We do not see evidence for the presence of accretion discs surrounding the collision products at the end of our

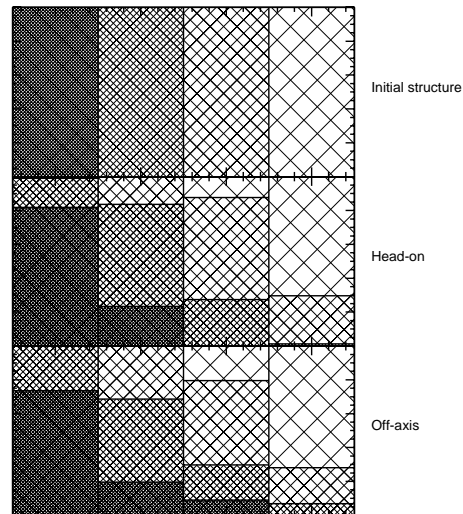


**Figure 3.** A plot of where the mass now in the collision product discussed above originally came from. The four columns in each plot represent four equally spaced mass bins. The darkest hatching represents material that came from the inner quarter of the parent stars, whilst the widest hatching represents material which came from the outer quarter of the parent stars. Shown are two blue straggler models, a head-on collision and an off-axis collision. As can be seen, the innermost quarter of the blue straggler is composed primarily of processed material from the parent stars. This indicates that the blue straggler will have a shorter lifespan than a main sequence star of equivalent mass.

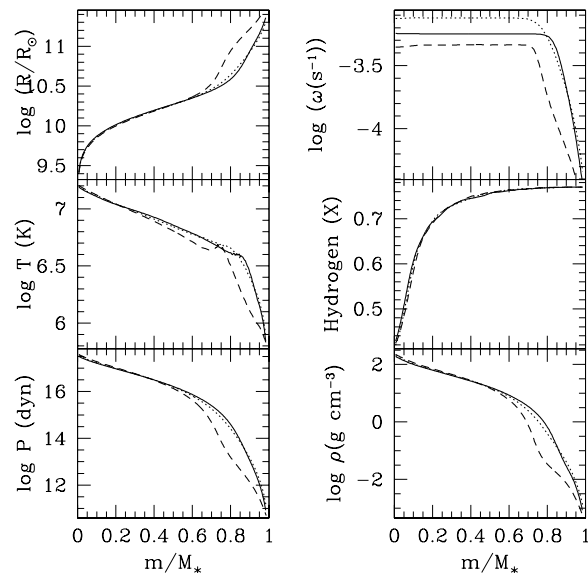


**Figure 4.** Structure of off-axis collision product for a collision between two  $0.6 M_{\odot}$  stars, with an impact parameter of  $0.25$  (solid line),  $0.5$  (dotted line) and  $1.0$  (dashed line).

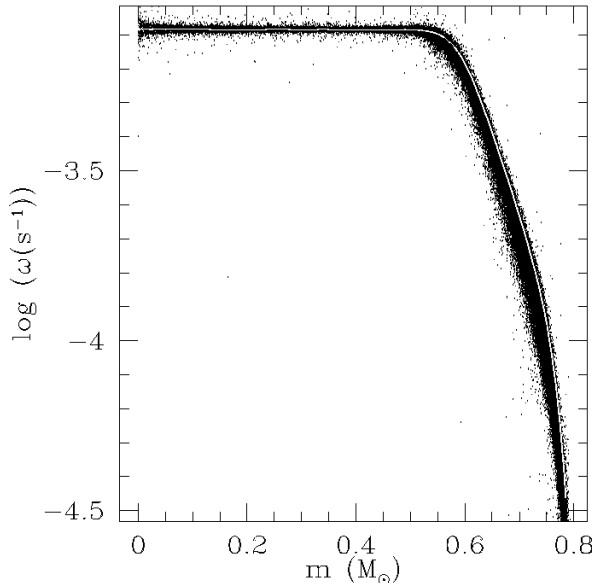


**Figure 5.** Angular velocity as a function of mass fraction for a collision between two  $0.4 M_{\odot}$  stars, with an impact parameter of 1.0. The dots show the results for each SPH particle, and the solid line is the average.

simulations for any combination of parent masses and impact parameter. This is in disagreement with the findings of Benz & Hills (1987). They collided two equal-mass  $n=1.5$  polytropes with a variety of impact parameters and velocities, and found that discs form in many of their collisions. The collisions which correspond most closely to the globular cluster collisions we are modelling have  $v_{\infty} = 0$ , and they give disc masses between 3 and 10% of the mass of system for impact parameters between 0.31 and  $0.953 R_1 + R_2$ , where  $R_1$  and  $R_2$  are the radii of the impacting stars.

The difference between our results and those of Benz & Hills (1987) may be related to a problem of definition. Most of our off axis simulations result in stars which are significantly flattened by rotation, and have rather oblate density contours at large distances from the star flattened in the  $z$  direction. (The stars are rotating about the  $z$  axis). However, none of the density contours have an axis ratio which is extreme enough to be called a disc. In fact, these results look similar in content to figure 9 of Benz & Hills (1987), in which their accretion disc is approximately as thick as the (flattened) radius of the central star. It is also possible that the presence of a disc might have been a numerical artifact caused by the lower resolution of the earlier simulations. Although we haven't seen direct evidence for a disc around the merged object, there is some material which is bound to the central object, although not apparently part of the blue straggler. Perhaps this material could eventually go on to form a disc around the central object.

### 3 EVOLUTION OF COLLISION PRODUCTS

With the SPH simulations completed, the next task is to perform the evolution of the models. Our SPH models showed, as in previous work, that they had too much angular mo-

mentum to contract down to the main-sequence. If these collision products are going to form some portion of the blue straggler population seen in globular clusters, they need a method of losing some of this angular momentum.

#### 3.1 Mass and angular momentum loss

Let us consider what is likely to happen to the blue straggler as it contracts down toward the main-sequence. As the star contracts it has to conserve angular momentum, so material is forced to rotate about the rotation axis faster. As this happens the star becomes deformed, becoming somewhat oblate. It is here that a new mechanism might be able to take effect. We know that the star can contract down to the point where it reaches its break up speed. At this point we could get mass loss as surface material becomes unbound from the star. This mass loss could do one of two things: it could take angular momentum away to infinity, thus reducing the angular momentum of the merged object, or alternatively it might form a disc around the star. If the star then has a strong magnetic field (which seems reasonable for most of the stars produced in the collisions detailed here as they are rapidly rotating) then it is possible for the disc and star to become locked, thus spinning down the star. Or the same magnetic field could be locked to the freely flowing material thus providing a torque in the same way as a stellar wind.

We need to examine how these two effects will alter the spin of the star if we are to incorporate their effects in the stellar evolution code.

##### 3.1.1 Disc locking

Let us first look at the effects of disc locking. The prescription that we have used follows on from the work of Armitage & Clarke (1996). The torque on a star from an annulus of a magnetically locked accretion disc, of width  $\Delta R$  is related to the transfer of angular momentum through magnetic stresses:

$$\Gamma_{\text{annulus}} = B_{\phi} B_z R^2 \Delta R \quad (1)$$

where  $B_z$  is the vertical component of the magnetic field at a distance  $R$  from the star and  $B_{\phi}$  is the toroidal component of the magnetic field. These two magnetic components may be expressed as:

$$B_z = \frac{\mu}{R^3} \quad (2)$$

where  $\mu$  is the stellar dipole moment. Livio & Pringle (1992) give the toroidal component as:

$$B_{\phi} = B_z \left( \frac{\Omega(R) - \Omega_{\star}}{\Omega(R)} \right) \quad (3)$$

where  $\Omega$  is the angular velocity of the Keplerian disc and  $\Omega_{\star}$  is the angular velocity of the star<sup>1</sup>.

The torque on the star will produce a change in its angular momentum, thus:

<sup>1</sup> This relation breaks down near the co-rotation radius, at this point  $B_{\phi} \approx B_z$

$$\begin{aligned} \frac{dJ}{dt} &= \Gamma_{\text{annulus}} \\ &= \frac{\mu^2}{R^4} \left( \frac{\Omega(R) - \Omega_\star}{\Omega(R)} \right) \Delta R \end{aligned} \quad (4)$$

and a change in the angular momentum of the body will alter its rotation rate:

$$\frac{dJ}{dt} = \Omega_\star \frac{dI_\star}{dt} + I_\star \frac{d\Omega_\star}{dt} \quad (5)$$

$$\frac{d\Omega_\star}{dt} = \frac{1}{I_\star} \left( \Gamma_{\text{annulus}} - \Omega_\star \frac{dI_\star}{dt} \right) \quad (6)$$

To get a proper estimate of the torque from the entire disc we have to integrate Eqn. 1 over the extent of the disc using the definitions of Eqn.s 2 and 3. If we assume that it extends from some inner radius  $R_{\text{in}}$  out to infinity then we get:

$$\Gamma_{\text{disc}} = \frac{\mu^2}{3} \left( \frac{1}{R_{\text{in}}^3} - \frac{2\Omega_\star}{(GM_\star R_{\text{in}}^3)^{\frac{1}{2}}} \right) \quad (7)$$

Thus the spin down rate of the star is now given by:

$$\frac{d\Omega_\star}{dt} = \frac{1}{I_\star} \left[ \frac{\mu^2}{3} \left( \frac{1}{R_{\text{in}}^3} - \frac{2\Omega_\star}{(GM_\star R_{\text{in}}^3)^{\frac{1}{2}}} \right) - \Omega_\star \frac{dI_\star}{dt} \right] \quad (8)$$

This expression indicates that the rate of spin down of the star is independent of the mass of the disc. Once we have a substantial disc we will get a braking torque on the star and it will always lead to the same reduction in the angular velocity of the star. This is in agreement with the results of Armitage & Clarke (1996).

If the material surrounding the merged object that was discussed in Section 3 does collapse down to form a disc, then it would have the same effects as the disc that has been postulated in this section.

### 3.1.2 Locking to out-flowing material

In previous sections we have explicitly stated that we do not have large convection zones on the surface of any of the collisional products. This has thus apparently ruled out a torque associated with stellar wind braking.<sup>2</sup> However, we know that the collisional product will contract and spin up. This will eject material from the stars surface, whilst not strictly a wind in the conventional sense, there is no apparent reason why this material cannot become locked to

<sup>2</sup> In a normal main-sequence star, if we are to lose angular momentum through a stellar wind, we require a deep surface convection zone. This is because angular momentum transport processes within the star are very slow. We rely on dynamical motions in the convection zone to speed up the transport of angular momentum around the star. However, the magnetic field of these merged objects is likely to be very high because of their rapid rotation (see Eqn. 18). Thus, it is likely that the star and field are tightly locked. Hence, as a torque is applied to the magnetic field, the whole star suffers the same torque and it is spun down.

the magnetic field as it moves away from the star and thus produce a braking torque.

To examine how this torque will break the rotation of the star, we first start off with the mass continuity equation:

$$\dot{m} = 4\pi R^2 \rho v \quad (9)$$

where  $\dot{m}$  is the mass loss from the star, or equivalently the mass flux of the wind-like material across a surface,  $v$  is the wind speed (which will be some multiple of the escape velocity of the star) and  $\rho$  is the density of the wind-like material.

We now look for pressure balance between the gas pressure and the magnetic pressure. This will give us the Alfvén radius for the star.

$$\rho_{\text{ra}} v_{\text{ra}}^2 = \frac{B_r^2(R_{\text{ra}})}{8\pi} \quad (10)$$

If we look at an open field line configuration, we may replace  $B_r$  with:

$$B_r = B_o \left( \frac{R_\star}{R} \right)^2 \quad (11)$$

If we now substitute Eqn.s 9 and 11 into Eqn. 10 we get:

$$R_{\text{ra}} = \frac{B_o R_\star^2}{\sqrt{2\dot{m}v}} \quad (12)$$

then simply setting the velocity of the wind to be the escape velocity from the surface of the star the Alfvén radius may be expressed as:

$$R_{\text{ra}} = B_o R_\star^{\frac{9}{4}} \dot{m}^{-\frac{1}{2}} m_\star^{-\frac{1}{4}} \frac{1}{(8G)^{\frac{1}{4}}} \quad (13)$$

If we the equate the angular momentum loss from the star to be the same as the angular momentum carried away by the wind once it has reached the Alfvén radius, one can say:

$$\frac{dJ}{dt} = \dot{m} \Omega_\star R_{\text{ra}}^2 \quad (14)$$

then once we substitute Eqn. 13 into the above we get:

$$\frac{dJ}{dt} = B_o^2 R_\star^{\frac{9}{2}} m_\star^{-\frac{1}{2}} \Omega_\star \frac{1}{(8G)^{\frac{1}{2}}} \quad (15)$$

This agrees with the results of Verbunt (1984).

Then by using Eqn. 6 we can get the spin down rate for the star:

$$\frac{d\Omega_\star}{dt} = \frac{1}{I_\star} \left[ B_o^2 R_\star^{\frac{9}{2}} m_\star^{-\frac{1}{2}} \Omega_\star \frac{1}{(8G)^{\frac{1}{2}}} - \Omega_\star \frac{dI_\star}{dt} \right] \quad (16)$$

One can make an estimate on the likely evolution of the radius of the blue straggler by using this torque. As we know, the torque will slow the star down and this will allow the star to contract to smaller and smaller radii until an equilibrium is reached. If we assume that the star is initially rotating at some fraction of its maximum rotation rate:

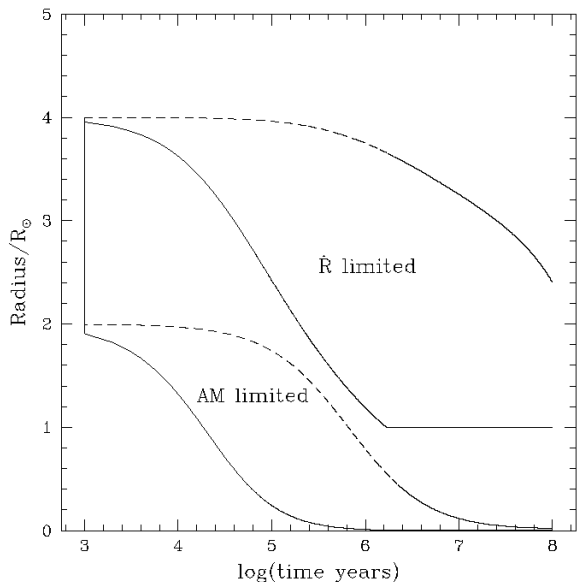


**Figure 6.** Evolution of the radius of the blue straggler as a function of time. The first two lines (labelled  $\dot{R}$ ) represent how the radius of the blue straggler would evolve if it were solely dependent on the angular momentum losses within the star. The solid line represents angular momentum losses due to wind braking, whilst the dashed line represents the effects of having a disc. In reality the star will shrink by more than this, as its radius is also dependent on the cooling of the star. The point where it can shrink to is limited by its angular momentum. The lower two lines on the plot show the smallest radius that the star can shrink to with the angular momentum that it has at a particular time step. The evolution of a blue straggler will lie somewhere in between the two encompassing lines.

$$\Omega_* = f \sqrt{\frac{GM_*}{R_*^3}} \quad (17)$$

then we can calculate the minimum size that the star can have as a function of time. This is plotted in Fig. 6. For this figure and the following, we are looking at a representative collision product with a mass of  $1 M_\odot$ , an initial radius of  $4 R_\odot$ , and an initial rotation rate where  $f = 0.707$ . We also assumed a magnetic field that had an initial value of 200 Gauss and varied with time as :

$$B = B_o \left( \frac{P_o}{P} \right)^2 \quad (18)$$

(following Armitage & Clarke (1996)), and a mass loss rate of  $10^{-10} M_\odot/\text{yr}$ , although the form of the graph is actually largely independent of  $\dot{m}$ . In the plot we have shown two sets of lines. The uppermost set represent the evolution of radius if it were solely dependent on the change in angular momentum of the star. The lower set represent the minimum radius that the star can contract to with the angular momentum that it has at a particular time step. As can be seen, we quickly lose sufficient angular velocity to allow the blue straggler to contract down via either angular momentum loss method. Once the star has contracted to its desired radius, the loss of angular momentum will continue,

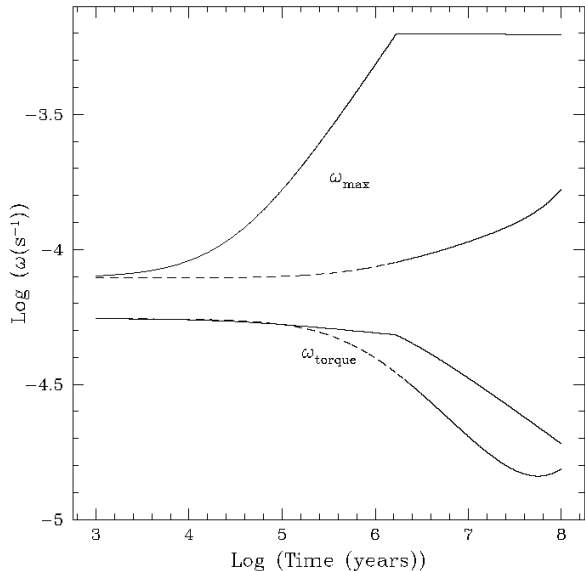


**Figure 7.** The spin evolution of one of the blue straggler stars. The solid lines represent the effects of angular momentum loss through a wind, whilst the dashed lines represent angular momentum loss through locking to a disc. The top two lines represent the maximum  $\omega$  that the model could have at a particular time if its radius was dominated by angular momentum losses (i.e. it followed the upper lines in Fig. 6). The lower two lines represent the  $\omega$  calculated for the models using Eqns. 8 and 16. As can be seen, both forms of angular momentum loss have very similar effects on the spin of the star, and rapidly take it below its critical velocity.

but now the star will maintain its radius and spin more slowly. In Fig. 7 we show the spin evolution of the same blue straggler. The lower set of lines represent the  $\omega$  that the star has because of the torque applied to the star. The upper set of lines represents the maximum  $\omega$  that a model can have at a particular time step if its radius is dominated by the angular momentum losses, i.e. the radius of the star follows the upper-most set of lines in Fig. 6. As can be seen, both forms of angular momentum loss have similar effects on the star, spinning it down to lower rotational velocities.

### 3.2 A detailed evolutionary calculation for an off-axis collision product with angular momentum loss

We chose one collision product to model in detail using a stellar evolution code, including the effects of rotation and the angular momentum loss methods described above. Angular momentum transport inside the star and the thermal contraction of the star are additional mechanisms which could substantially impact the evolution of the blue straggler. In this section, we look at those effects for one representative case, the M66Q case ( $M_1 = 0.6 M_\odot$ ,  $M_2 = 0.6 M_\odot$ ,  $r_p = 0.25R_1 + R_2$ ).

### 3.2.1 *The Stellar Evolution Code*

Our stellar evolution calculations are performed with YREC. YREC is a one-dimensional code, in which the star is divided into shells along surfaces of constant gravitational plus rotational potential. The code solves the equations of stellar structure with the Henyey technique, and follows the rotational evolution with the formalism of Endal & Sofia (1976). Guenther *et al.* (1992) give a detailed description of the physics implemented in the evolution code. We used the same opacities, equation of state and model atmospheres as in Sills *et al.* (1997). The free parameters in the code (the mixing length and parameters that set the efficiency of angular momentum transport and rotational chemical mixing) are set by calibrating a solar mass and solar metallicity model to the sun.

Rotation is treated by evaluating physical quantities on equipotential surfaces rather than the spherical surfaces usually used in stellar models. The hydrostatic equilibrium and radiative transport equations contain terms that account for the lack of spherical symmetry in the rotating star. A number of rotational instabilities that transport angular momentum and material within the star are followed, including dynamical shear (Pinsonneault *et al.* 1989), meridional circulation (von Zeipel 1924), secular shear (Zahn 1974), and the Goldreich-Schubert-Fricke instability (Goldreich & Schubert 1967; Fricke 1968). Angular momentum transport and the associated chemical mixing are treated as diffusion processes, with diffusion coefficients that account for each active mechanism within unstable regions of the star. The diffusion coefficients are proportional to circulation velocities, which have been estimated by Endal & Sofia (1978). In addition to the internal rearrangement of angular momentum, angular momentum also can be drained from an outer convection zone through a magnetic wind, using the formalism given by Chaboyer *et al.* (1995). For a detailed description of the implementation of rotation in YREC, see Pinsonneault *et al.* (1989).

### 3.2.2 *Conversion to YREC Format*

The results of the three-dimensional SPH simulations were converted to one-dimensional models suitable to use as starting models for YREC. The specific entropy of the particles (defined as  $A = P/\rho^\gamma$ ), their chemical abundances and their specific angular momentum were averaged over surfaces of constant effective potential (gravitational plus rotational), and binned into approximately 100 bins. With the entropy and angular momentum profiles given, the structure of the rotating remnant is uniquely determined in the formalism of Endal & Sofia (1976) by integrating the general form of the equation of hydrostatic equilibrium. To do so, we implement an iterative process in which initial guesses for the central pressure and angular velocity are refined upon until a self-consistent YREC model is converged upon. For more details of the conversion between SPH results and stellar evolution models, see Sills *et al.* (1997, 2001).

### 3.2.3 *Early Evolution and Treatment of Angular Momentum Loss*

Immediately after the collision, the collision products have large radii and are quite far out of thermal equilibrium. Their early evolution is dominated by a contraction back to the main sequence. Since they are not homogeneous pre-main sequence stars, however, this contraction produces a track (for non-rotating stars) which moves down the middle of the HR diagram rather than on the cool Hayashi track. Rotating stars have an additional complication. These stars are rotating quite rapidly (surface rotation velocities of  $\sim 300 - 700 \text{ km s}^{-1}$ , depending on the star), although less than their surface break-up velocities at this point. As the star contracts, its surface rotation rate increases due to angular momentum conservation. The radius shrinks as well, which increases the break-up velocity, but unfortunately for the star, the angular momentum wins. Shortly after the collision, the star is rotating faster than its break-up velocity, and mass will be thrown off of the star. This should lead to a self-regulating process where the star continues to rotate at its break-up velocity, shedding mass as required to maintain that rate.

Standard stellar evolution codes do not usually allow the star to lose mass. We have implemented a mass loss routine in YREC which removes mass from a surface convection zone if one exists, or from the entire star if one does not. All our blue straggler candidates fall in the latter category. We calculate what fraction of the star is rotating at higher than its local break-up velocity at a given time, and then (to ensure numerical stability of our models) remove that fraction from each of the shells in the star. We assume that the mass loss occurs instantaneously, so that the changes to radius, temperature, density, and pressure of each shell will occur during the evolutionary time step following the mass loss. We need to remove the angular momentum that leaves the star with the mass. We do this by assuming that the profile of angular momentum as a function of mass fraction in the star remains the same as before, but is truncated at the new outer edge of the star. The same procedure is used to determine the new composition of each shell, so that we are not artificially removing helium directly from the core of the star. This new configuration is allowed to evolve for another timestep (typically on order 100 years at this early stage of the evolution) and then the process is repeated.

It is plausible to assume that the mass that is lost from the star can do one of two things: either it is lost from the star to infinity immediately, or it remains in a disc around the star for some time. If the star has a magnetic field, the star can become locked to the disc so that its surface rotation rate is determined by the rotation rate of the disc. This disc-locking is assumed to be important in the rotational evolution of pre-main sequence stars (Konigl 1991; Sills, Pinsonneault & Terndrup 2000; Barnes, Sofia, & Pinsonneault 2001), and may well be applicable to blue stragglers (although see Matt & Pudritz (2004)). We have added a module to the stellar evolution code which allows this disc-locking to be turned on for a given amount of time (which is a user-set parameter). The surface rotation rate of the star is fixed to be the surface rotation rate immediately after the mass was lost. If this

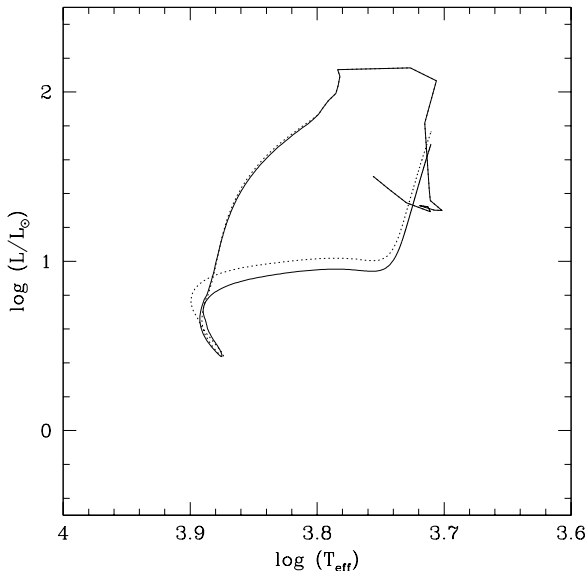


**Figure 8.** Evolutionary tracks in the Hertzsprung-Russell diagram for the M66Q collision, with (solid line) and without (dotted line) disc-locking.

module is turned on, the disc-locking turns on after the star has lost at least  $0.1 M_{\odot}$ .

### 3.2.4 Results

We ran two evolutionary calculations. The collision product was evolved until it threw off the minimum mass required for disc-locking to turn on. Then, we either allowed the star to continue evolving without the disc-locking, or locked the star to the disc for 5 million years. The lifetimes for pre-main sequence discs are thought to range between 0 and 10 million years (Strom *et al.* 1989).

The evolutionary tracks of the collision products with disc-locking (solid lines) and without (dotted lines) are presented in Fig. 8. Initially the star lost  $0.10 M_{\odot}$  during its super-critical rotation period. The final angular momentum after the mass loss was  $9.0 \times 10^{49} \text{ g cm}^2 \text{ s}^{-1}$ , and after the star had been locked to a disc for 5 Myr, its total angular momentum was  $1.5 \times 10^{49} \text{ g cm}^2 \text{ s}^{-1}$  (i.e. the star loses  $\sim 80\%$  of its angular momentum during the 5 Myr disk-locking period). Note that the stars lose  $\sim 90\%$  of their initial angular momentum during the mass loss phase. The material at the outer edge of the star has very large specific angular momentum, so a little bit of mass can remove a lot of angular momentum.

While both stars initially begin their post-collision evolution in the lower right portion of this diagram, the star that was locked to a disc follows a fairly normal evolutionary track. This star is still significantly brighter than a normal star of the same mass and shows some evidence of rotational mixing and modification of evolutionary track and lifetime. The star that was not locked to a disc (dotted line) mixes more hydrogen to the core and helium to the surface. Its evolutionary track is slightly bluer and brighter, and its main sequence lifetime is slightly longer than the disk-locked star.

In Fig. 9, we plot the surface rotation velocity in  $\text{km s}^{-1}$

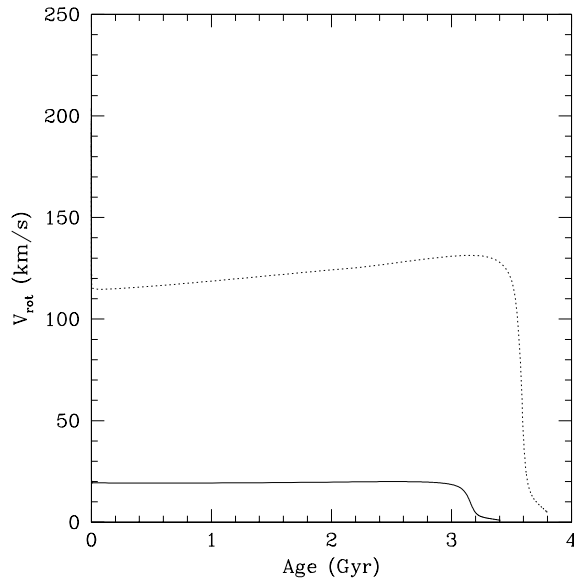


**Figure 9.** Rotation rate as a function of time for the M66Q collision, with (solid line) and without (dotted line) disc-locking. The shaded region shows the current range of detected rotation rates for blue stragglers in globular clusters:  $155 \pm 55 \text{ km s}^{-1}$  (BSS-19 in 47 Tuc, Shara *et al.* (1997)) and  $200 \pm 50 \text{ km s}^{-1}$  (BSS-17 in M3, De Marco *et al.* (2004)).

as a function of time for the M66Q collision, with the solid line showing the star which was locked to a disc, and the dotted line for the star which was allowed to evolve freely after it lost mass. The difference in surface rotation rates is quite apparent, and directly reflects the amount of angular momentum which was carried away by the disc. Rotation rates of  $125 \text{ km/s}$  are quite fast for stars of  $1 M_{\odot}$  (our Sun rotates at  $\sim 2 \text{ km s}^{-1}$ ), but are not completely unreasonable given the observed rotation rate of a few blue stragglers in a globular cluster. The ordinate of this graph gives the range of observed rotation rates (Shara *et al.* 1997; De Marco *et al.* 2004).

An interesting effect of rotation in stars is the amount of rotationally-induced mixing that can occur. Since rotating stars are subject to a variety of thermodynamic and hydrodynamic instabilities, more mixing of material can occur than that caused by convection. This mixing, particularly of hydrogen to the core and helium to the surface, is responsible for the extended lifetime of the rotating stars, and is shown in Fig. 10. This plot of surface helium abundance as a function of time for the M66Q collision shows that neither star ever becomes fully mixed, but that the non-disk-locked star does show some rotationally-induced mixing over its main sequence lifetime.

Other elements also trace this rotation mixing. The CNO elements, for example, show strong changes as CNO processed material is dredged up from the nuclear burning regions to the surface. These changes are shown in Fig. 11. As with the helium abundance, the star which was not locked to a disc shows a much stronger signature of rotational mixing than the star with a disc. The clearest evidence of this mixing shows up in the  $^{12}\text{C}/^{13}\text{C}$  ratio, which deviates from the canonical main sequence value of 90 fairly early in its

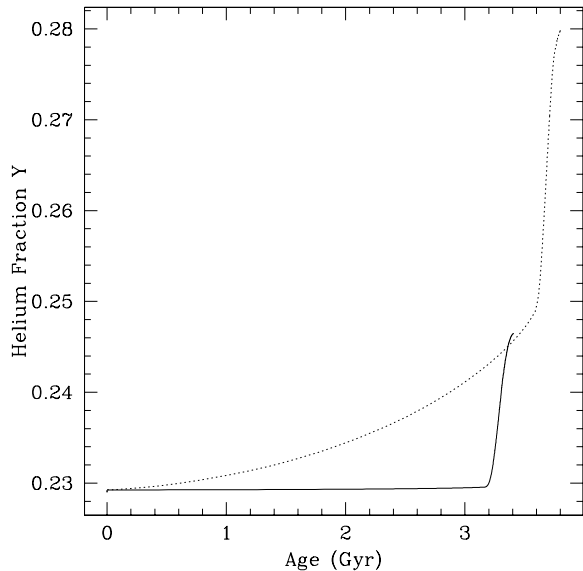


**Figure 10.** Helium abundance as a function of time for the M66Q collision, with (solid line) and without (dotted line) disc-locking.

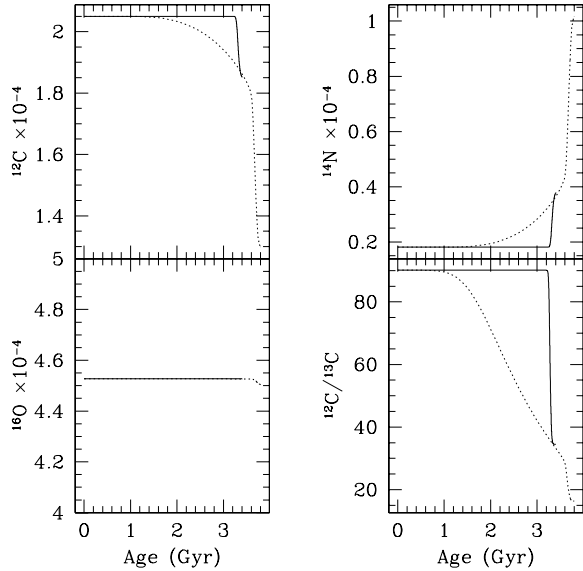


**Figure 11.** Surface composition as a function of time for the M66Q collision, with (solid line) and without (dotted line) disc-locking.

main sequence lifetime. This ratio may be a crucial diagnostic for determining the rotational histories of blue stragglers.

The choice of disc lifetime, at 5 Myr, was based on our understanding of discs around pre-main sequence stars and was somewhat arbitrary. We ran an identical simulation with a 10 Myr disc to test the extreme of the plausible range. The majority of the angular momentum was lost from the star in the first few Myr, and so extending the disc lifetime did not make a substantial difference to the star’s evolution. The total angular momentum of the blue straggler was 1.493

$\times 10^{49} \text{ g cm}^2 \text{ s}^{-1}$  after 10 Myr (compared to  $1.498 \times 10^{49} \text{ g cm}^2 \text{ s}^{-1}$ ) and at an age of 2 Gyr, the star with the 10 Myr disc had  $v \sin i = 19.7 \text{ km s}^{-1}$  compared to  $19.8 \text{ km s}^{-1}$  for the star with a 5 Myr disc. Therefore, we conclude that the disk needs to survive for only a few Myr in order to slow the star down substantially.

An additional level of arbitrariness was setting the mass of the disk beyond which disk locking occurs. To test this, we locked our star to its disk as soon as it lost any mass at all. Under this scenario, the star’s surface rotation rate was fixed at  $\omega = 5.9e - 5 \text{ rad s}^{-1}$  for 5 Myr starting almost immediately after the collision. This produced a significantly different evolution than that shown in figure 8. The star loses a total of  $0.42 M_{\odot}$  rather than  $0.1 M_{\odot}$ . This is understandable – if we wait to lock the star’s rotation rate, then the star has more time to contract towards the main sequence. This thermal contraction rate is largest early on. As the star contracts, it is more likely to exceed its maximum rotation speed for a given  $\omega$ , and so the star ends up losing much more mass. Interestingly, the final rotation rate of this new low-mass star is approximately the same as the star which was locked to a disk after it lost  $0.1 M_{\odot}$ : about  $20 \text{ km/s}$ . Therefore, the disk mass at which locking can occur could change the total mass of the blue straggler, but apparently has less impact on its rotational properties. We argue that a disk mass of  $0.1 M_{\odot}$  is reasonable based on our understanding of disk-locking in pre-main sequence stars.

We also tested our assumption that the star is locked at the surface rotation rate immediately after the mass is lost. The star is rotating quite rapidly at this point, so this assumption can be taken to be a reasonable upper limit to the rotation rate of the star. If the star manages to lose more mass than we assumed, or if it is locked to the disk at a lower surface rotation rate, than the blue straggler will be rotating even slower than we have shown in the previous calculations. We ran the same simulations as discussed above, except that at the time when the star was locked to its disk, we locked it at one-fifth of the current surface rotation rate. The factor of 5 was chosen to represent a reasonable reduction in rotation rate. We ran the simulations with both a 5 Myr and a 10 Myr disk. As expected, the total angular momentum of the system after the disk-locking episode was approximately a factor of 5 lower than in the original calculations (5.2 times lower for the 5 Myr disk and 4.97 times for the 10 Myr disk). The surface rotation rates were lower by a factor of  $\sim 4$ .

## 4 DISCUSSION AND CONCLUSIONS

We used SPH to simulate stellar collisions relevant for the formation of blue stragglers in globular clusters. Our results were the same as seen in other papers, with the possible exception of the lack of discs. We believe that the higher resolution of our calculations and the use of realistic stellar models (rather than polytropes) is the root of the discrepancy between our simulations and those of Benz & Hills (1987). It should also be noted that the discs observed around blue stragglers by De Marco *et al.* (2004) have masses much lower than the particle masses in our SPH simulations, and so the simulations and observations are not in disagreement.

We have shown that magnetic locking to either a disc or to outflowing material would produce sufficient angular mo-

mentum loss to avoid complete break-up of the blue straggler. We have shown that if the star is locked to a disc of material via a magnetic field, enough angular momentum is lost for the star to evolve along a basically normal, but brighter, evolutionary track. If, on the other hand, the star is allowed to lose mass but is not locked to a disc, it continues to evolve at a significant fraction of its surface break-up velocity. Substantial amounts of hydrogen and helium are mixed throughout the star via the rotational instabilities, and the star follows a path in the colour-magnitude diagram which runs up the zero-age main sequence. The star becomes very hot and very blue, and has a greatly extended main sequence lifetime.

We see some very bright blue stragglers in some clusters (M3, NGC 6752, NGC 6397). In other clusters, the blue stragglers are not particularly bright, nor are they constrained to lie on the zero-age main sequence (Ferraro *et al.* 2003). Instead, they are all to the red of the ZAMS. Therefore, the highly rotational models (i.e. those without disc locking) do not match most of the observations well. Either most blue stragglers are locked to a disc and therefore evolve more like non-rotating stars, or stellar collisions are not the dominant creation mechanism for these stars. It is possible that the brightest, bluest blue stragglers in clusters are indeed rotating rapidly, and that that is the cause of their position in the colour-magnitude diagram. However, the stars in question are not as bright or as blue as the predictions from the no-disc models, so we conclude that the disc-locking mechanism, or some similar angular momentum loss mechanism, must be at work during the blue straggler formation process.

Is it reasonable to assume that the collision product can be locked to a disc? Low mass stars all have magnetic fields, so if the field can be maintained and remains coherent during the stellar collision, then the product should also have a field of the appropriate strength. It is difficult to understand how the magnetic field could be completely removed from the stellar material during the collision, although the stirring up of stellar material may indeed weaken it. More work is needed to determine if the magnetic field of the collision product will be coherent enough at the end of the collision to provide the locking required.

There are a number of observational tests which will shed some direct light on the nature of blue stragglers as rotators. The most obvious is measurements of rotation rates of blue stragglers from spectra, as was done for BSS 19 in 47 Tuc (Shara *et al.* 1997). HST STIS spectra have been taken for blue stragglers in a number of clusters, but the reductions have not yet been published. The early indications are that the blue stragglers are rotating very slowly, less than  $v \sin i = 50 \text{ km s}^{-1}$ . (Shara, private communication, 2003). These spectra will also be incredibly useful for determining surface gravity values for blue stragglers, which lead to mass determinations. A comparison of derived mass with location in the colour-magnitude diagram will allow us to determine if blue stragglers have evolutionary tracks like normal main sequence stars, or if they are more like the rotational evolutionary tracks presented in this paper. Particularly for the brighter blue stragglers, the masses will allow us to distinguish between rotationally-modified evolutionary tracks and stars with masses more than twice the turnoff mass. An additional spectral diagnostic for rotation

is the abundances of a variety of elements, particularly the CNO elements and helium. The rotationally-induced mixing signatures can be particularly strong and fairly unambiguous, although the CNO abundances at the surface of a binary merger product are yet to be determined. Since collisional blue stragglers should live at the centres of dense clusters, observing them spectroscopically will be quite challenging and points to the use of the Hubble Space Telescope and ground-based adaptive optics systems. However, there are now more and more telescopes equipped to perform this kind of work, which would significantly reduce the level of uncertainty about these interesting and useful members of globular clusters.

## 5 ACKNOWLEDGMENTS

AS is supported by NSERC. TAD acknowledges a PPARC studentship. MBD is supported by a research fellowship from the Swedish Royal Academy of Sciences and PPARC funding for theoretical astronomy at the University of Leicester. The computations reported here were performed using the UK Astrophysics Fluids Facility (UKAFF) and the SHARCNet facilities at McMaster University.

## REFERENCES

- Adams, T., Davies, M. B., Sills, A. 2004, *MNRAS*, 348, 469  
 Armitage, P. J., Clarke, C. J. 1996, *MNRAS*, 280, 458  
 Bailey, V. C. & Davies, M. B. 1999, *MNRAS*, 308, 257  
 Barnes, S., Sofia, S., & Pinsonneault, M. 2001, *ApJ*, 548, 1071  
 Bate, M.R., Bonnell, I.A., Price, N.M., 1995, *MNRAS*, 277, 362  
 Benz, W., 1990, in Buchler J. R., ed., The Numerical Modeling of Nonlinear Stellar Pulsations: Problems and Prospects. Kluwer, Dordrecht, p. 269  
 Benz, W., Hills, J. G. 1987, *ApJ*, 323, 614  
 Chaboyer, B., Demarque, P., Pinsonneault, M. H. 1995, *ApJ*, 441, 865  
 Davies, M. B., Piotto, G., de Angeli, F. 2004, *MNRAS*, 349, 129  
 De Marco, O., Lanz, T., Ouellette, J. A., Zurek, D., & Shara, M. M. 2004, *ApJL*, 606, L151  
 Endal, A. S., Sofia, S. 1976, *ApJ*, 210, 184  
 Endal, A. S., Sofia, S. 1978, *ApJ*, 220, 279  
 Ferraro, F. R., Sills, A., Rood, R. T., Paltrinieri, B., Buonanno, R. 2003, *ApJ*, 588, 464  
 Fricke, K. 1968, *Zs. Ap.*, 68, 317  
 Goldreich, P., Schubert, G. 1967, *ApJ*, 150, 571  
 Guenther, D. B., Demarque, P., Pinsonneault, M. H., Kim, Y.-C., 1992, *ApJ*, 392, 328  
 Konigl, A., 1991, *ApJ*, 370, L39  
 Livio, M., Pringle, J. E. 1992, *MNRAS*, 259, 23P  
 Lombardi, J. C., Jr., Rasio, F. A., Shapiro, S. L., 1996, *ApJ*, 468, 767  
 Matt, S. & Pudritz, R. E. 2004, *ApJL*, 607, L43  
 Monaghan, J.J, 1992, *ARA&A*, 30, 543  
 Peterson, R. C., Carney, B. W. Latham, D. W. 1984, *ApJ*, 279, 237

- Pinsonneault, M. H., Kawaler, S. D., Sofia, S., Demarque, P. D. 1989, *ApJ*, 338, 424
- Preston, G. W., Sneden, C. 2000, *Aj*, 120, 1014
- Rahunen, T. 1981, *A&A*, 102, 81
- Sandquist, E., Bolte, M., Hernquist, L., 1997, *ApJ*, 477, 335
- Shara, M., Saffer, R., Livio, M. 1997, *ApJL*, 489, L59
- Sills, A., Baily, C. D. 1999, *ApJ*, 513, 428
- Sills, A., Lombardi, J. C., Jr., Baily, C. D., Demarque, P. D., Rasio, F. A., Shapiro, S. L., 1997, *ApJ*, 487, 290
- Sills, A., Pinsonneault, M. H., Terndrup, D. M., 2000, *ApJ*, 534, 335
- Sills, A., Faber, J. A., Lombardi, J. C., Jr., Rasio, F. A., Warren, A. R., 2001, *ApJ*, 548, 323
- Sills, A., Adams, T., Davies, M. B., Bate, M. R. 2002, *MNRAS*, 332, 49
- Strom, K. M., Strom, S. E., Edwards, S., Cabrit, S., Skrutskie, M. F. 1989, *Aj*, 97, 1451
- Tassoul, J. 2000, *Stellar rotation / Jean-Louis Tassoul*. Cambridge ; New York : Cambridge University Press, 2000. (Cambridge astrophysics series ; 36)
- Verbunt, F. 1984, *MNRAS*, 209, 227
- von Zeipel, H. 1924, *MNRAS*, 84, 665
- Zahn, J.-P. 1974 in *IAU Symposium 59: Stellar Instability and Evolution*, ed. P. Ledoux, A. Noels & A. W. Rodgers (Dordrecht:Reidel) p. 185